

Charge-order phase transition in the quasi one-dimensional organic conductor (TMTTF)₂NO₃

Lena Nadine Majer · Björn Miksch ·
Guilherme Gorgen Lesseux · Gabriele Untereiner ·
Martin Dressel

Received: date / Accepted: date

Abstract Low-dimensional organic conductors show a rich phase diagram, which has, despite all efforts, still some unexplored regions. Charge ordered phases present in many compounds of the (TMTTF)₂X family are typically studied with their unique electronic properties in mind. An influence on the spin arrangement is, however, not expected at first glance. Here, we report temperature and angle dependent electron spin resonance (ESR) measurements on the quasi one-dimensional organic conductor (TMTTF)₂NO₃. We found that the (TMTTF)₂NO₃ compound develops a peculiar anisotropy with a doubled periodicity (*ab'*-plane) of the ESR linewidth below about $T_{CO} = (250 \pm 10)$ K. This behavior is similar to observations in the related compounds (TMTTF)₂X ($X = \text{PF}_6$, SbF_6 and AsF_6), where it has been attributed to relaxation processes of magnetically inequivalent sites in the charge-ordered state. For the structural analogous (TMTTF)₂ClO₄, known for the absence of charge order, such angular dependence of the ESR signal is not observed. Therefore, our ESR measurements lead us to conclude that a charge-order phase is stabilized in the title compound below $T_{CO} \approx 250$ K.

Keywords Charge-order state · Low-dimensional organic conductor · Electron spin resonance

PACS 75.10.Pq · 71.70.Ej · 75.25.-j · 76.30.-v

1. Physikalisches Institut
Universität Stuttgart
Pfaffenwaldring 57
70569 Stuttgart
Germany

Corresponding author: Lena Nadine Majer
E-mail: lena-nadine.majer@pi1.physik.uni-stuttgart.de

Guilherme Gorgen Lesseux
Current address: Iowa State University and Ames Laboratory, Ames, IA 50011, USA

Declarations

Funding Financial support by the Deutsche Forschungsgemeinschaft (DFG), grant DR228/52-1, is thankfully acknowledged.

Conflicts of interest The authors declare that they have no conflict of interest.

Availability of data and materials The data that support the findings of this study are available from the corresponding author, Martin Dressel, upon reasonable request.

Authors' contributions All authors contributed to the study conception and design. Crystals have been grown by Gabriele Untereiner, ESR measurements and data analysis were performed by Lena Nadine Majer, Björn Miksch and Guilherme Gorgen Lesseux. The first draft of the manuscript was written by Lena Nadine Majer and all authors commented on previous versions of the manuscript. All authors read and approved the final manuscript.

1 Introduction

Low-dimensional organic conductors have drawn attention for decades because they show a rich phase diagram with a variety of interesting ground states [1]. Due to the reduced dimensionality of the electronic structure and rather strong electronic correlations, these materials exhibit unusual thermodynamic, transport, optical, and magnetic properties. The charge and spin degrees of freedom in the Bechgaard and Fabre salts can be tuned from localized to itinerant by changing the anions as well as external parameters such as temperature or pressure. This can lead to various phases in the charge and spin sector, such as charge order, antiferromagnetic phases, spin density wave and even superconductivity [2, 3, 4, 5]. Here we focus on the (TMTTF)₂X family, where TMTTF denotes tetramethyltetrathiafulvalene and X stands for a monovalent anion – here specifically on $X^- = \text{NO}_3^-$. Using electron spin resonance (ESR) as a local probe of electronic and magnetic properties, we yield information on the phase transitions as a function of temperature.

One-dimensional organic conductors can be described by the Hubbard model. The (TMTTF)₂X compounds are nominally 3/4-filled systems, dimerization along the chains however leads to a half-filled conduction band. Hence the compounds are supposed to exhibit metallic behavior, but strong electron-electron interaction can cause localization of the electrons, depending on the competition between electronic correlations modeled by an on-site Coulomb repulsion U and the bandwidth W . In addition, most members of the Fabre family undergo a phase transition to a symmetry broken ground state at low temperatures. In the present case, one expects that inter-site Coulomb repulsion V drives the systems into a charge-ordered phase; i.e. an alternating arrangement of charge rich and charge poor molecules leads to localization of carriers. Since in the (TMTTF)₂X crystals the stacks are slightly dimerized on stoichiometric grounds, one does not necessarily expect a doubling of the unit cell [2]. As continuously stressed by Pouget and collaborators [6, 7, 8, 9], the interaction with the anions cannot be ruled out and any change in the molecular charge pattern will affect the structural arrangement and vice versa.

The magnetic properties of (TMTTF)₂X salts have been intensely studied by ESR during the last years [10, 11, 12, 13, 14, 15, 16, 17, 18, 19]. In the case of centro-symmetric anions, such as PF_6^- , SbF_6^- and AsF_6^- , Yasin *et al.* observed that the symmetry of the magnetic degrees of freedom are broken when charge order occurs on the molecular stack [16, 17]. Dutoit *et al.* confirmed these observations and pointed out that also the counter-ions X are involved, in accord with previous observations [20, 21, 22, 23]. Since two magnetically inequivalent sites are present below the charge-ordering temperature, the ESR spectra should show two distinct signals. However, exchange coupling mixes the lines, resulting in a significant increase of the linewidth. A charge-ordered state influences the relaxation mechanism leading to a change in the anisotropy of the linewidth; the g -tensor remains unaffected. In the absence of charge order, the linewidth typically follows the sinusoidal anisotropy of the g -value with 180° symmetry. When charge order sets in below T_{CO} , the periodicity of the linewidth doubles, as observed when rotating the magnetic field in the ab' -plane, normal to the long axis of the molecule. This anisotropy is enhanced with the magnetic field H_0 oriented in a direction between the stacking axis a and the perpendicular direction b' due to anisotropic Zeeman interaction [24] resulting from relaxation processes between the magnetically inequivalent sites on the adjacent stacks in the charge-ordered state [16].

In the case of non centro-symmetric anions, the situation is more complex: in addition to a charge-order transition, some of the salts exhibit anion ordering at low temperatures, leading to a tetramerization of the stacks [25]. For (TMTTF)₂ClO₄, on the other hand, the anions order at $T_{\text{AO}} = 73$ K without any sign of charge-order [5]. There is an ongoing discussion

whether (TMTTF)₂NO₃ undergoes a charge-order transition upon cooling. DC conductivity shows a maximum at 210 K below which the sample exhibits an insulating behavior [26]. Based on a small feature of the asymmetry of the ESR lineshape, Coulon *et. al.* conclude that charge order occurs around 110 K [18]. At $T_{AO} = 50$ K the system shows an anion-ordering phase transition leading to the formation of spin singlets. The exponential decrease of the ESR intensity evidences the opening of a spin gap [27, 18]. Here we present results on (TMTTF)₂NO₃ revealing a change in anisotropy periodicity of the ESR linewidth below around 250 K, as previously found for other members of the TMTTF family at their charge-ordering temperature [16]. From the similarity to the behavior in the Fabre salts with centrosymmetric anions [16] we conclude a charge ordering in the title compound.

2 Experimental details

The measurements of the electron spin resonance (ESR) were performed on a continuous-wave X-band spectrometer (Bruker EMXplus) in a frequency range of 9 to 10 GHz. The spectrometer is equipped with a goniometer. A continuous He-gas flow cryostat (Oxford instruments, ESR 900) allows us to cool from ambient temperature to $T = 4$ K. The experiments were performed on single crystals of (TMTTF)₂NO₃ grown by standard electrochemical procedure [28, 29]. The specimens used for our measurements have a typical size of $2.5 \times 0.5 \times 0.1$ mm³. The triangular anion NO₃ is not centro-symmetric. The TMTTF salts have a triclinic symmetry, the planar TMTTF molecules extend along the *c*-axis and are stacked in *a*-direction. The *g*-tensor is oriented in *a*, *b'*, and *c** direction, where *b'* is the projection of *b* perpendicular to the *a*-axis, and *c** normal to the *ab*-plane.

3 Results

The room-temperature anisotropy of *g*-value and linewidth ΔH of (TMTTF)₂NO₃ is plotted in Fig. 1. The maximum values of *g* and ΔH are found with $H_0 \parallel c^*$. Along the stacking direction *a* the values are smallest, whereas for $H_0 \parallel b'$ intermediate values are observed. Note, the linewidth always follows the behavior of the ellipsoidal *g*-tensor, i.e. maxima and minima alternate when rotating in steps of 90°. These findings are similar to the anisotropy observed in other compounds of the (TMTTF)₂*X* family. The anomalously large rotation of the *g*-tensor upon cooling associated with the CO transition observed for (TMTTF)₂*X* (*X* = PF₆, SbF₆) [14] is not present in (TMTTF)₂NO₃. Only a minor reorientation of $\sim 3^\circ$ between room temperature and $T = 4$ K is observed similar to the case of (TMTTF)₂Br [14].

For elevated temperatures the line is slightly asymmetric due to considerable conductivity; therefore a Dysonian lineshape is used for the analysis [30]. The signal measured along the crystal axes can be well described by a single Dysonian line in the entire studied temperature-range. In the charge-ordered state one might expect two distinguishable lines due to the magnetically inequivalent sites on the adjacent stacks. However, exchange interaction can mix the lines making them indistinguishable; this results in an increased linewidth [16]. For (TMTTF)₂NO₃ only slight hints of two lines are observed, as displayed in Fig. 2(c). Using a single line, the maximum and minimum of the spectrum can be fitted almost perfectly. We conclude that the exchange coupling dominates, as previously found for other members of the TMTTF family [16]. For all further results, we used a single Dysonian line to fit the ESR spectra.

Fig. 2(a) displays the observed ab' -plane anisotropy of the linewidth for different temperatures. The regular ellipsoidal anisotropy of the linewidth $\Delta H(\theta)$ can be fitted by

$$\Delta H(\theta) = \sqrt{\Delta H_a^2 \cos^2(\theta) + \Delta H_{b'}^2 \sin^2(\theta)}. \quad (1)$$

here ΔH_a and $\Delta H_{b'}$ denote the linewidths for the external field H_0 aligned parallel to the crystallographic a -axis and b' -axis, respectively [16]. The room-temperature behavior is well described by equation (1) as shown in Fig. 2(a). Upon cooling, at around 250 K, the angular behavior of the linewidth in the ab' -plane starts to develop additional contributions around the diagonal directions at 45° and 135° , and increasingly deviates from the description by equation (1); below $T = 100$ K the anisotropy changes significantly. Additional maxima develop at the positions of 45° and 135° , exceeding the linewidth along the b' direction. As the linewidth anisotropy starts to deviate from the behavior described by equation (1) and indicate an onset of a doubled periodicity component (see Fig. 2(a), $T = 200$ K), an additional contribution is required to describe the angular dependence observed in (TMTTF)₂NO₃. The doubling of the periodicity is accounted for by adding the term

$$\Delta H_{\text{doubl.}}(\theta) = \Delta H_{\text{mod}} \sin^2(2\theta) \quad (2)$$

to equation (1). The amplitude of the additional contribution to the linewidth along the 45° direction is given by ΔH_{mod} .

Below $T \sim 250$ K, the angular-dependent linewidth of (TMTTF)₂NO₃ was fitted by a sum of equations (1) and (2). Fig. 3(a) shows the temperature dependence of the fit parameters. The finite value of ΔH_{mod} suggests that a charge-order state already exists in this temperature range.

Our results resemble the behavior observed in (TMTTF)₂SbF₆, (TMTTF)₂AsF₆ and (TMTTF)₂PF₆, which undergo a charge-order transition upon cooling below T_{CO} [16, 17].

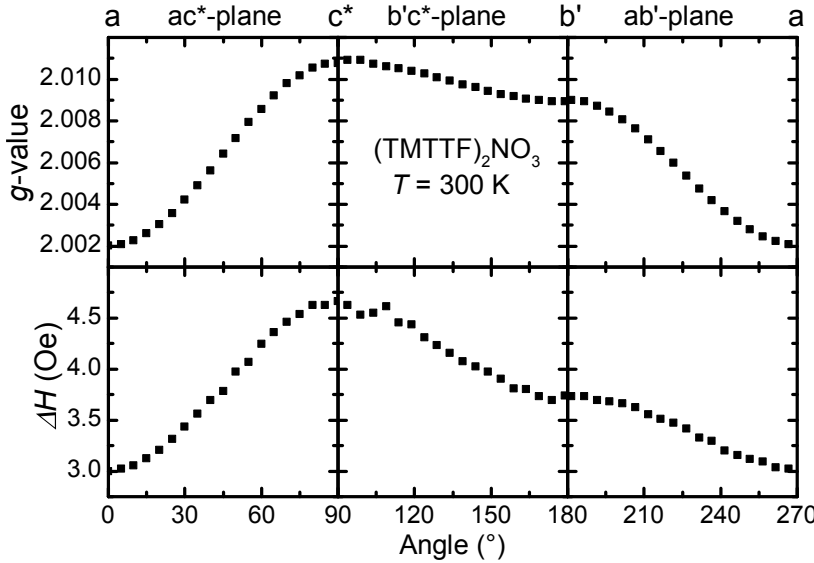


Fig. 1 Anisotropy of ESR g -value and linewidth of (TMTTF)₂NO₃. The measurements were performed at room temperature by rotating the magnetic field H_0 in the ab' , ac^* and $b'c^*$ -planes. The maximum g -value and linewidth is found along the c^* -direction; the smallest along the a -axis.

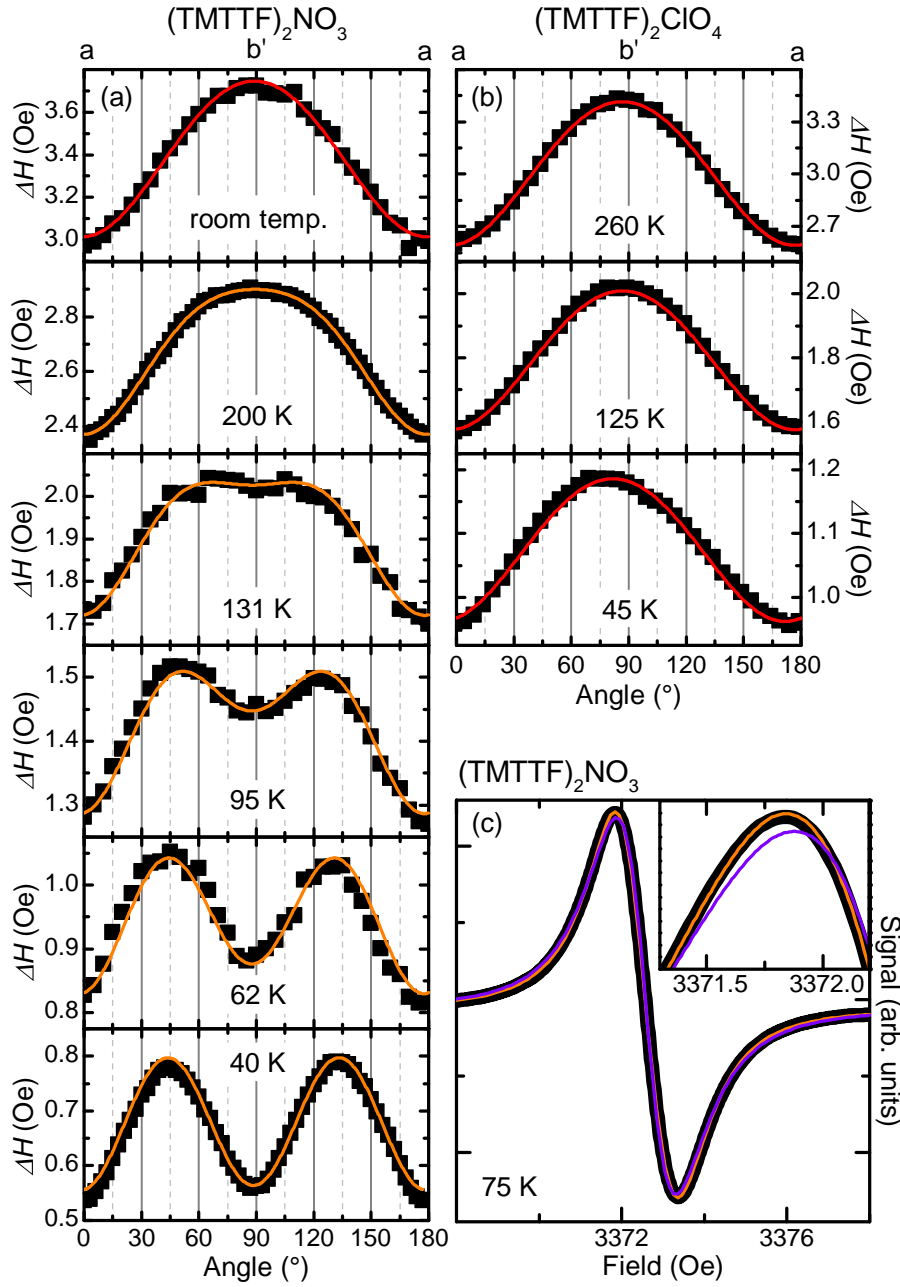


Fig. 2 (a) The linewidth of a $(\text{TMTTF})_2\text{NO}_3$ crystal measured in the ab' -plane at different temperatures. At $T = 300$ K the data can be fitted by Eq. (1), corresponding to the red line. For lower temperatures, $T = 200$ K, 131 K, 95 K, 62 K and 40 K, a sum of Eqs. (1) and (2) have to be used; these are represented by the orange lines. (b) For comparison, the angle dependence of the linewidth of a $(\text{TMTTF})_2\text{ClO}_4$ sample in the ab' -plane is plotted for $T = 260$ K, 125 K and 45 K, respectively. In this case, the signal can always be described by Eq. (1). The obtained fit parameters are summarized in Tab. 1. (c) The $T = 75$ K ESR signal of $(\text{TMTTF})_2\text{NO}_3$ in the diagonal ab' -direction. The inset magnifies the maximum. The purple line was obtained by one Dysonian line, while the orange line is fitted by two Dysonian. Although the difference is small, the orange line fits better.

Table 1 Fit parameters of the angle-dependent linewidth of (TMTTF)₂ClO₄. The measurement was performed in the ab' -plane. The rotation at $T = 260$ K, 125 K and 45 K can be well described by Eq. (1), as illustrated in Fig. 2(b).

(TMTTF) ₂ ClO ₄	260 K	125 K	45 K
ΔH_a [Oe]	2.6 ± 0.1	1.6 ± 0.1	1.0 ± 0.1
$\Delta H_{b'}$ [Oe]	3.4 ± 0.1	2.0 ± 0.1	1.2 ± 0.1

It is interesting to note that this doubled periodicity of the linewidth was only observed in Fabre salts with centro-symmetric anions, while in the case of linear anions, such as (TMTTF)₂SCN, a totally different behavior was found. The triangular symmetry of the NO₃⁻ anion also allows a doubling of the periodicity at lower temperatures. From our ESR results we conclude that (TMTTF)₂NO₃ exhibits a charge-order transition leading to additional relaxational processes due to anisotropic Zeeman interaction, similar to the behavior in compounds with centro-symmetric anions [16].

For comparison, we performed temperature and angular-dependent ESR measurements on (TMTTF)₂ClO₄ that is known to not develop to a charge-order phase at low temperatures [18]. As shown in Fig. 2(b), the overall behavior of the linewidth periodicity in the ab' -plane is temperature independent. It can be fitted using only equation (1). The resulting parameters of the fit are given in Tab. 1.

In Fig. 3 the temperature dependence of the g -value (b) and the linewidth ΔH (c) of (TMTTF)₂NO₃ is presented, as measured along the a and b' -direction and for 45° between a and b' (diagonal direction). The g -value measured along 45° is between the value along the a and b' -axes over the entire temperature range. In contrast, the value of the linewidth in the diagonal ab' -direction is only halfway between the value along the a and b' -axis for high temperatures. However at $T^* \approx 125$ K the linewidth in the diagonal direction of the ab' -plane becomes larger than along the a and b' directions. This confirms that in the 45° direction a further contribution to the linewidth exists as already shown with the fits to the angle-dependent measurements. However, already at a temperature of around $T = 250$ K the linewidth of the diagonal-direction ΔH_{diag} is larger than the value estimated by equation (1) using the measured values ΔH_a and $\Delta H_{b'}$, as indicated by the solid orange line in 3(c).

The temperature dependence of the linewidth $\Delta H(T)$ shows no distinct features along any crystallographic axes in contrast to the behavior observed for (TMTTF)₂SbF₆ and (TMTTF)₂AsF₆, where a clear kink has been found at the charge order temperatures [16]. The behavior resembles (TMTTF)₂PF₆: there at the charge-order transition at $T = 67$ K no kink becomes obvious. Only for the diagonal orientation a change in the slope of the derivative ($d(\Delta H_{\text{diag}})/dT$) is identified around $T_{\text{CO}} = (250 \pm 10)$ K, as indicated in the inset of Fig. 3(c). Hence, for our ESR data we suggest that (TMTTF)₂NO₃ is charge ordered below $T_{\text{CO}} \approx 250$ K.

Fig. 3 (d) shows the temperature dependence of the ESR intensity. The overall behaviour resembles the spin susceptibility of other (TMTTF)₂X compounds [10]. The intensity monotonically decreases upon cooling from room temperature to 4 K. Below the anion-ordering transition at around 50 K the chain dimerizes accompanied by the formation of spin singlets, leading to the observed exponential decay of the spin susceptibility [27, 18].

4 Conclusion

In summary we have performed angular and temperature dependent X-band ESR experiments on (TMTTF)₂NO₃ and (TMTTF)₂ClO₄ single crystals. The temperature evolution of the

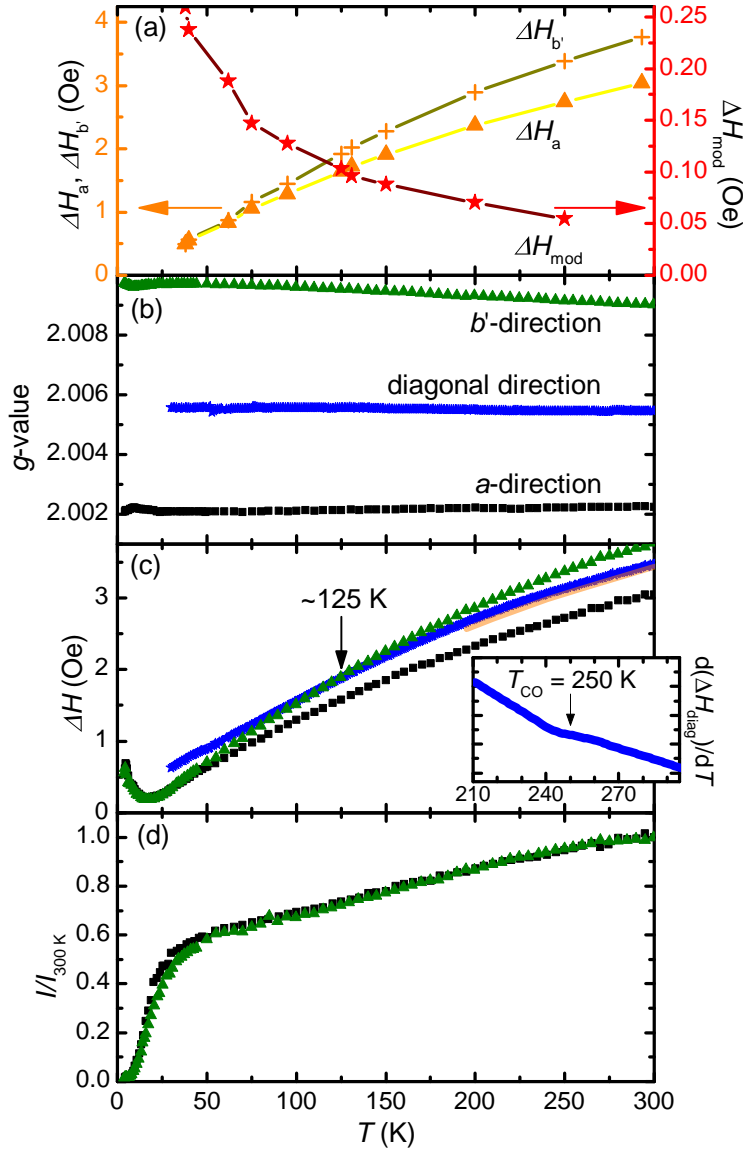


Fig. 3 (a) Fit parameters of the linewidth anisotropy of the (TMTTF)₂NO₃ compound at different temperatures. A sum of Eqs. (1) and (2) was fitted. Temperature dependent *g*-value (b) and linewidth ΔH (c) of (TMTTF)₂NO₃ measured by X-band ESR. Around $T = 125$ K, the linewidth in the diagonal direction crosses the linewidth for the *b'*-orientation. This is taken as indication that a charge-order transition is present in (TMTTF)₂NO₃. The orange line is the estimated ΔH_{diag} by Eq. (1) using the measured values ΔH_a and $\Delta H_{b'}$. The inset shows the derivative of the smoothed data for the linewidth in diagonal orientation. (d) ESR intensity for *a* and *b'*-orientation normalized to the room temperature value.

linewidth anisotropy in the ab' -plane for (TMTTF)₂NO₃ gives microscopic evidence for the stabilization of a charge ordered phase below $T_{CO} = (250 \pm 10)$ K for this compound.

Acknowledgements We are very grateful to Dr. Yohei Saito and Dr. Roland Rösslhuber for fruitful discussions.

References

1. A. Lebed (ed.), *The Physics of Organic Superconductors and Conductors* (Springer-Verlag, Berlin, 2008)
2. M. Dressel, *Naturwissenschaften* **94**(7), 527 (2007). DOI 10.1007/s00114-007-0227-1. URL <https://doi.org/10.1007/s00114-007-0227-1>
3. B. Köhler, E. Rose, M. Dumm, G. Untereiner, M. Dressel, *Phys. Rev. B* **84**, 035124 (2011). DOI 10.1103/PhysRevB.84.035124. URL <https://link.aps.org/doi/10.1103/PhysRevB.84.035124>
4. M. Dressel, M. Dumm, T. Knoblauch, M. Masino, *Crystals* **2**(2), 528 (2012). DOI 10.3390/cryst2020528. URL <https://www.mdpi.com/2073-4352/2/2/528>
5. R. Rösslhuber, E. Rose, T. Ivek, A. Pustogow, T. Breier, M. Geiger, K. Schrem, G. Untereiner, M. Dressel, *Crystals* **8**(3), 121 (2018). URL <https://www.mdpi.com/2073-4352/8/3/121>
6. J.P. Pouget, S. Ravy, *J. Phys. (Paris) I* **6**, 1501 (1996)
7. J.P. Pouget, *Crystals* **2**, 466 (2012). DOI 10.3390/cryst2020466
8. J.P. Pouget, P. Foury-Leylekian, P. Alemany, E. Canadell, *phys. stat. sol. (b)* **249**, 937 (2012). DOI 10.1002/pssb.201100750
9. J.P. Pouget, P. Alemany, E. Canadell, *Mater. Horiz.* **5**, 590 (2018). DOI 10.1039/C8MH00423D. URL <http://dx.doi.org/10.1039/C8MH00423D>
10. M. Dumm, A. Loidl, B.W. Fravel, K.P. Starkey, L.K. Montgomery, M. Dressel, *Phys. Rev. B* **61**, 511 (2000). DOI 10.1103/PhysRevB.61.511. URL <https://link.aps.org/doi/10.1103/PhysRevB.61.511>
11. M. Dumm, A. Loidl, B. Alavi, K.P. Starkey, L.K. Montgomery, M. Dressel, *Phys. Rev. B* **62**, 6512 (2000). DOI 10.1103/PhysRevB.62.6512. URL <https://link.aps.org/doi/10.1103/PhysRevB.62.6512>
12. T. Nakamura, *J. Phys. Soc. Jpn.* **72**(2), 213 (2003). DOI 10.1143/JPSJ.72.213. URL <https://doi.org/10.1143/JPSJ.72.213>
13. C. Coulon, R. Clérac, *Chem. Rev.* **104**(11), 5655 (2004). DOI 10.1021/cr030639w. URL <https://doi.org/10.1021/cr030639w>
14. K. Furukawa, T. Hara, T. Nakamura, *J. Phys. Soc. Jpn.* **78**(10), 104713 (2009). DOI 10.1143/JPSJ.78.104713. URL <https://doi.org/10.1143/JPSJ.78.104713>
15. B. Salameh, S. Yasin, M. Dumm, G. Untereiner, L. Montgomery, M. Dressel, *Phys. Rev. B* **83**, 205126 (2011). DOI 10.1103/PhysRevB.83.205126. URL <https://link.aps.org/doi/10.1103/PhysRevB.83.205126>
16. S. Yasin, B. Salameh, E. Rose, M. Dumm, H.A. Krug von Nidda, A. Loidl, M. Ozerov, G. Untereiner, L. Montgomery, M. Dressel, *Phys. Rev. B* **85**, 144428 (2012). DOI 10.1103/PhysRevB.85.144428. URL <https://link.aps.org/doi/10.1103/PhysRevB.85.144428>
17. M. Dressel, M. Dumm, T. Knoblauch, B. Köhler, B. Salameh, S. Yasin, *Adv. Condens. Matter Phys.* **2012**, 398721 (2012). URL <https://doi.org/10.1155/2012/398721>
18. C. Coulon, P. Foury-Leylekian, J.M. Fabre, J.P. Pouget, *The Eur. Phys. J. B* **88**(4), 85 (2015)
19. C.E. Dutoit, A. Stepanov, J. van Tol, M. Orio, S. Bertaina, *J. Phys. Chem. Lett.* **9**(18), 5598 (2018). DOI 10.1021/acs.jpclett.8b02070. URL <https://doi.org/10.1021/acs.jpclett.8b02070>
20. D.S. Chow, F. Zamborszky, B. Alavi, D.J. Tantillo, A. Baur, C.A. Merlic, S.E. Brown, *Phys. Rev. Lett.* **85**, 1698 (2000). DOI 10.1103/PhysRevLett.85.1698. URL <https://link.aps.org/doi/10.1103/PhysRevLett.85.1698>
21. P. Foury-Leylekian, S. Petit, G. Andre, A. Moradpour, J. Pouget, *Physica B* **405**(11, Supplement), S95 (2010). DOI <http://dx.doi.org/10.1016/j.physb.2009.11.043>
22. M. de Souza, P. Foury-Leylekian, A. Moradpour, J.P. Pouget, M. Lang, *Phys. Rev. Lett.* **101**, 216403 (2008). DOI 10.1103/PhysRevLett.101.216403. URL <https://link.aps.org/doi/10.1103/PhysRevLett.101.216403>
23. E. Rose, M. Dressel, *Physica B* **407**(11), 1787 (2012). DOI <https://doi.org/10.1016/j.physb.2012.01.030>. URL <http://www.sciencedirect.com/science/article/pii/S092145261200035X>
24. A. Bencini, D. Gatteschi, *Electron Paramagnetic Resonance of Exchange Coupled Systems* (Springer-Verlag, Berlin, 1990)

25. A. Pustogow, T. Peterseim, S. Kolatschek, L. Engel, M. Dressel, *Phys. Rev. B* **94**, 195125 (2016). DOI 10.1103/PhysRevB.94.195125. URL <https://link.aps.org/doi/10.1103/PhysRevB.94.195125>
26. C. Coulon, P. Delhaes, S. Flandrois, R. Lagnier, E. Bonjour, J. Fabre, *J. Phys. (Paris)* **43**(7), 1059 (1982). DOI 10.1051/jphys:019820043070105900. URL <https://doi.org/10.1051/jphys:019820043070105900>
27. R. Moret, J.P. Pouget, R. Comès, K. Bechgaard, *J. Phys. (Paris) Colloq.* **44**(C3), 957 (1983). DOI 10.1051/jphyscol/1983118. URL <https://doi.org/10.1051/jphyscol/1983118>
28. B. Liautard, S. Peytavin, G. Brun, M. Maurin, *J. Phys. (Paris)* **43**(10), 1453 (1982). DOI 10.1051/jphys:0198200430100145300. URL <https://doi.org/10.1051/jphys:0198200430100145300>
29. B. Liautard, S. Peytavin, G. Brun, M. Maurin, *Acta Cryst. Sec. B* **38**(10), 2746 (1982). DOI 10.1107/S0567740882009844. URL <https://doi.org/10.1107/S0567740882009844>
30. F.J. Dyson, *Phys. Rev.* **98**, 349 (1955). DOI 10.1103/PhysRev.98.349. URL <https://link.aps.org/doi/10.1103/PhysRev.98.349>